

Towards the inclusion of NLO EW corrections in the MiNLO method in Drell-Yan processes

Filippo Belloni,^a Mauro Chiesa,^a Carlo Oleari,^{b,c} Emanuele Re^{b,c,1}

^a*INFN, Sezione di Pavia, via Bassi 6, 27100 Pavia, Italy*

^b*Università degli Studi di Milano - Bicocca, Piazza della Scienza 3, 20126 Milano, Italy*

^c*INFN, Sezione di Milano - Bicocca, Piazza della Scienza 3, 20126 Milano, Italy*

E-mail: filippo.belloni@pv.infn.it, mauro.chiesa@pv.infn.it,
carlo.oleari@mib.infn.it, emanuele.re@mib.infn.it

ABSTRACT: In this paper we present the first application of the MiNLO method to the calculation of QED NLO corrections to the production of a neutral vector boson in Drell-Yan processes. We consider only the case of initial-state radiation, when the Z boson decays into neutrinos. We illustrate the abelianization procedure of the MiNLO formulae and discuss the impact that it has on the differential cross section. We then propose a variant of the MiNLO formulae in order to circumvent some of the problems that arise when dealing with QED emissions. Since this is a case study, we use ad-hoc parton distribution functions and a larger value of the electromagnetic coupling constant, in order to emphasize potential discrepancies with respect to the expected behavior of the MiNLO formulae. We quantify the uncertainties connected with the proposed method, also for a the physical value of the electromagnetic coupling. The study presented here is a necessary first step towards incorporating full electroweak effects into the MiNNLO_{PS} framework.

KEYWORDS: NLO QED corrections, MiNLO, resummation.

¹On leave of absence from LAPTh, Université Grenoble Alpes, Université Savoie Mont Blanc, CNRS, F-74940 Annecy, France.

Contents

1	Introduction	1
2	The MiNLO formalism for QCD	5
3	The MiNLO formalism for QED	8
3.1	The running of the electromagnetic coupling	8
3.2	The color factors	9
3.3	The QED Sudakov peak and the implications for the MiNLO formulation	10
3.4	The QED evolution of parton distribution functions	11
4	Implementation of the QED MiNLO formulae	12
5	Validation and results	13
6	Conclusions	21

1 Introduction

The charged and neutral Drell–Yan (DY) processes constitute one of the cornerstones of precision physics at hadron colliders. Notably, owing to its clean experimental signature and high production rate, neutral current (NC) Drell-Yan production provides stringent tests of the Standard Model (SM) and plays a crucial role in precision measurements, such as the extraction of electroweak (EW) parameters and the calibration of detector response. On a similar note, the charged-current (CC) production is crucial, among other reasons, for extracting the mass of the W boson (M_W), which is one of the fundamental parameters of the SM, and whose precise knowledge is of significant importance to test the theory at the quantum level.

The accumulated statistics at the LHC, together with the effort put forth by the experimental collaborations to reduce systematic uncertainties, have pushed the precision of these measurements to an unprecedented level (see e.g. Refs. [1–3] for the weak mixing angle $\sin^2 \theta_W^{\text{eff}}$, or [4, 5] for the W -boson mass), making theoretical uncertainties a non-negligible component of the total error budget. This is particularly relevant in view of the High-Luminosity LHC (HL-LHC) era, where, for instance, the target precision for $\sin^2 \theta_W^{\text{eff}}$ is 15×10^{-5} , requiring, in turn, the theoretical simulation of the forward-backward asymmetry to be under control at the level of few 10^{-4} in the peak region. In this context, the need for increasingly accurate theoretical predictions and reliable Monte Carlo simulation tools has become particularly pressing.

For instance, in measurements based on the template fit method, theoretical predictions are used to generate templates as functions of the parameters to be extracted, and any approximation in the modeling (from the truncation of the perturbative series to parametric uncertainties) directly propagates into systematic uncertainties of theoretical origin. This is especially relevant for electroweak precision measurements based on NC and CC DY processes.

Although electroweak corrections are typically subleading at hadron colliders, as a consequence of the hierarchy between the couplings α and α_s with $\alpha \sim \alpha_s^2$, it is well known that they induce phenomenologically significant effects. Photon radiation, particularly from the final state, can lead to sizable distortions of key kinematic distributions and induce radiative return effects in the presence of resonances. Furthermore, at high invariant masses, EW Sudakov logarithms and photon-induced subprocesses significantly enhance the impact of electroweak corrections (see Ref. [6] for a comprehensive overview of the main features of electroweak corrections). For the Drell-Yan process, NLO EW corrections have been available for a long time [7–17], and the effects of multiple photon radiation have been extensively studied [14, 16, 18–20]. These NLO EW corrections are currently available in both dedicated Monte Carlo codes [11, 12, 14–16, 21–28] and automated tools [29–32]. Tuned comparisons of the theory predictions for CC and NC DY processes obtained with some of these tools can be found in Ref. [33]. In most of these programs, the weak corrections are combined additively with NLO QCD results. More recently, next-to-next-to-leading order (NNLO) QCD corrections have been combined with NLO EW effects in codes such as FEWZ [34] and MATRIX [35–37]. Furthermore, several tools incorporate the contribution of the leading fermionic corrections beyond NLO, while the full two-loop EW corrections, expressed in terms of form factors, have been made available in the GRIFFIN library [38]. The exclusive exponentiation of QED correction for DY processes within the YFS framework is implemented in the event generator KKMC-hh [39–43]. Significant progress has also been achieved in the computation of mixed QCD-EW corrections, which have been shown to reach the percent level for observables relevant to present and future LHC analyses, competing with residual perturbative uncertainties from higher-order QCD effects [44–62]. Progress on the two-loop electroweak corrections to NC DY is documented in [63]. In addition to fixed-order calculations, significant progress has recently been achieved in incorporating QED effects into the resummation of large logarithmic corrections to the vector-boson transverse momentum spectrum. Mixed QCD \otimes QED resummation at next-to-leading logarithmic accuracy (NLL) + NLO was developed in Refs. [64, 65] for on-shell W and Z production, and in Ref. [66] for off-shell dilepton production with massive fermions. The resummation of mixed QCD \otimes QED at next-to-next-to-leading-logarithmic (NNLL) accuracy for NC DY was performed in [67].¹

¹Related work on mixed QCD \otimes QED Sudakov resummation can also be found in Ref. [68].

The steadily increasing experimental accuracy requires theoretical predictions that consistently incorporate higher-order radiative corrections beyond QCD and, ideally, combine fixed-order (FO) calculations with parton shower (PS) simulations. While NLO QCD corrections and their matching to parton showers (NLO+PS) are by now standard and essentially automated [29, 69–79], the matching of FO electroweak effects with PS has received comparatively less attention. While several studies have explored the approximate inclusion of EW corrections within higher-order QCD frameworks [80–83], the consistent matching of NLO electroweak corrections to parton showers remains, to date, limited to only a few specific results [84–92]. Such studies have so far been primarily focused on Drell-Yan production processes, and, often, the matching is obtained simultaneously for QCD and EW corrections in the POWHEG framework. By consequence, such Monte Carlo generators also include, within some approximation, the factorizable subset of the mixed QCD-EW corrections to inclusive DY production. In particular, the code in Ref. [84] was used to study the theory uncertainties from weak and mixed QCD-EW effects on the determination of the W -boson mass at the LHC [93].

At the same time, DY-based measurements are becoming increasingly differential with respect to kinematic variables such as the transverse momentum of the vector boson (p_T), which is known to be critically sensitive to QCD initial-state radiation (ISR) and plays a crucial role, for instance, in W -mass measurements. In current simulation strategies, EW effects are often included using tools that provide only leading-order accuracy in the description of the vector-boson transverse momentum, while the latter is modeled using higher-order QCD calculations that do not include EW corrections. This mismatch highlights the importance of developing simulation tools capable of simultaneously providing an accurate description of both inclusive observables and radiation-sensitive quantities, consistently combining state-of-the-art QCD and EW predictions. The development of event generators at this level of accuracy would require, among other ingredients, the inclusion of NLO EW corrections (and specifically NLO QED) not only for the inclusive Drell-Yan process, but also for the radiative process $DY + \mathcal{A}$, where \mathcal{A} denotes a resolved emission at $\mathcal{O}(\alpha)$, which can consist either of a photon or an (anti-)quark originating from an $\mathcal{O}(\alpha)$ splitting. The latter contribution is necessary to describe the p_T spectrum with NLO accuracy in the high transverse-momentum region. A further essential ingredient is the merging of NLO predictions for the inclusive process with those for the process featuring one resolved radiation. Despite the advanced technology developed for the DY process and the fact that electroweak corrections for $W/Z + \gamma$ and $W/Z + j$ are known² [99, 100], a unified framework capable of consistently describing both unresolved and resolved QED emission has been lacking so far.

²The issue of matching QCD corrections with parton showers in the presence of isolated photons has been addressed at NLO for the process $pp \rightarrow W(l\nu)\gamma$ and direct γ production in Refs. [94, 95] and at NNLO for $Z + \gamma$, $W + \gamma$, and $\gamma\gamma$ production in Refs. [96–98].

In this work, we take a first step towards addressing this issue by constructing an event generator that merges DY production including NLO QED corrections with DY plus one resolved QED radiation at NLO QED accuracy, employing the MiNLO method³ [101, 102]. The resulting computation achieves NLO accuracy in the resolved radiation regime, while simultaneously reproducing NLO predictions for inclusive DY observables. The MiNLO method was originally formulated to obtain predictions for the process $pp \rightarrow F + j$ (F being a colorless system) at NLO QCD accuracy, with the additional feature of recovering the NLO accurate results for the inclusive $pp \rightarrow F$ process, when observables inclusive with respect to radiation are considered. The algorithm served also as the starting point for the formulation of the MiNNLO method [103, 104], which allows simulating the $F + j$ process at NLO accuracy in QCD, while achieving NNLO accuracy for the inclusive $pp \rightarrow F$ process (NNLO+PS). Notably, the MiNNLO approach, and, *de facto*, MiNLO, was also generalized to the case of heavy colored final states, such as for $t\bar{t}$ production in hadronic collisions [105], as well as to other final states featuring two heavy quarks [106–108]. Other algorithms for the matching of NNLO QCD calculations to parton showers have been developed in [79, 109–111].

The adaptation of the MiNLO method to QED represents an essential step towards a unified treatment of QCD and electroweak corrections within modern event generators and lays the groundwork for future extensions aiming at NLO QCD + NLO EW accuracy (with matching to QCD and QED parton shower) for finite values of the vector boson p_T , and ultimately NNLO QCD + NLO EW precision (plus parton shower) for observables inclusive with respect to strong and electromagnetic radiation.

In the following sections, we will attempt to follow the original MiNLO formulation for QCD as closely as possible to highlight the new aspects and criticalities of its application to QED, using the $pp \rightarrow Z\mathcal{A} \rightarrow \nu\bar{\nu}\mathcal{A}$ process (where $\mathcal{A} = \{q, \bar{q}, \gamma\}$ and the initial-state particles can be quarks and photons) as a case study, in order to concentrate on a process with only initial-state radiation.⁴ At this stage, we will not make any attempt to interface our MiNLO process with a parton shower, since the result would be unphysical without the inclusion of the QCD radiation. In addition, current parton-shower tools for LHC physics are not designed to treat only QED emissions, without QCD effects.

The paper is organized as follows. In Sec. 2 we recall the formulation of the

³In Ref. [101] the improved MiNLO method proposed originally in [102] was dubbed MiNLO', in order to distinguish the two formulations. In the MiNLO' framework, one also recovers NLO accuracy, for observables inclusive with respect to the emitted radiation. In this paper, for ease of notation, we generically adopt the notation MiNLO instead of MiNLO'.

⁴This is the first step towards the more general case of massive charged-lepton production $pp \rightarrow Z\mathcal{A} \rightarrow \mu^+\mu^-\mathcal{A}$, where also final-state radiation is present, following the work done for $t\bar{t}$ production of Ref. [105].

MiNLO method for QCD. The key aspects and the main issues of the adaptation of the MiNLO algorithm to the case of QED corrections are discussed in Sec. 3, where we describe the treatment of the QED coupling constant and detail the abelianization of the MiNLO formulas as well as the treatment of the parton distribution functions. The position of the Sudakov peak is also discussed together with its consequences on the formulation of the method. We present the technical details of the implementation of our calculation in Sec. 4. The validation of the calculation and a discussion of the numerical results can be found in Sec. 5. Finally we give our conclusions in Sec. 6.

2 The MiNLO formalism for QCD

In this section, we recall the main formulae underlying the MiNLO method. We use the the notation of Ref. [103] for the QCD case, applied here to the $pp \rightarrow Z(\rightarrow \nu\bar{\nu}) X$ process at NLO accuracy in QCD, where X denotes the radiation against which the Z recoils. We will then extend the formalism to the case of QED corrections, illustrating all the issues related with the abelianization procedures.

Up to $\mathcal{O}(\alpha_s^2)$, the differential cross section as a function of the Born phase space for Z production, Φ_Z , and of the transverse momentum of the Z boson, p_T , can be written as⁵

$$\frac{d\sigma}{d\Phi_Z dp_T} = \frac{d\sigma^{\text{sing}}}{d\Phi_Z dp_T} + R_f(p_T), \quad (2.1)$$

where R_f contains terms that are non-singular in the small p_T limit and the singular differential cross section can be written as

$$\frac{d\sigma^{\text{sing}}}{d\Phi_Z dp_T} = \frac{d}{dp_T} \left\{ \exp[-\tilde{S}(p_T)] \mathcal{L}(p_T) \right\}, \quad (2.2)$$

where $\tilde{S}(p_T)$ is the Sudakov exponent and $\mathcal{L}(p_T)$ involves the parton luminosities, the Born squared amplitude for the production of the Z boson, the hard-virtual corrections and the collinear coefficient functions (see Ref. [103] for more details). We can further elaborate eq. (2.2) and write eq. (2.1) as

$$\frac{d\sigma}{d\Phi_Z dp_T} = \exp[-\tilde{S}(p_T)] D(p_T) + R_f(p_T), \quad (2.3)$$

where

$$D(p_T) \equiv -\frac{d\tilde{S}(p_T)}{dp_T} \mathcal{L}(p_T) + \frac{d\mathcal{L}(p_T)}{dp_T}. \quad (2.4)$$

The Sudakov exponent and its derivative are given by

$$\tilde{S}(p_T) = 2 \int_{p_T}^Q \frac{dq}{q} \left\{ A(\alpha_s(q)) \log \frac{Q^2}{q^2} + \tilde{B}(\alpha_s(q)) \right\}, \quad (2.5)$$

⁵For ease of notation, we do not indicate explicitly the Φ_Z dependence of \mathcal{L} and R_f .

and

$$\frac{d\tilde{S}(p_T)}{dp_T} = -\frac{2}{p_T} \left\{ A(\alpha_s(p_T)) \log \frac{Q^2}{p_T^2} + \tilde{B}(\alpha_s(p_T)) \right\}, \quad (2.6)$$

where Q is the virtuality of the Z boson. In the specific case of Drell-Yan production, the functions A and B , up to second order in α_s , have the following expressions

$$\begin{aligned} A(\alpha_s) &= \left(\frac{\alpha_s}{2\pi}\right) A^{(1)} + \left(\frac{\alpha_s}{2\pi}\right)^2 A^{(2)}, \\ \tilde{B}(\alpha_s) &= \left(\frac{\alpha_s}{2\pi}\right) B^{(1)} + \left(\frac{\alpha_s}{2\pi}\right)^2 \tilde{B}^{(2)}, \end{aligned} \quad (2.7)$$

where

$$\begin{aligned} A^{(1)} &= 2C_F, & B^{(1)} &= -3C_F, \\ A^{(2)} &= \left(\frac{67}{9} - \frac{\pi^2}{3}\right) C_A C_F - \frac{20}{9} C_F T_F n_f, \\ B^{(2)} &= \left(-\frac{17}{12} - \frac{11\pi^2}{12} + 6\zeta_3\right) C_A C_F \\ &\quad + \left(-\frac{3}{4} + \pi^2 - 12\zeta_3\right) C_F^2 + \left(\frac{1}{3} + \frac{\pi^2}{3}\right) C_F T_F n_f \\ \tilde{B}^{(2)} &= B^{(2)} + 2\pi \beta_0 H + 2\zeta_3 (A^{(1)})^2, & \beta_0 &= \frac{11C_A - 4T_F n_f}{12\pi}, \end{aligned} \quad (2.8)$$

H being the hard-virtual coefficient function

$$H = \left(-8 + \frac{7}{6}\pi^2\right) C_F. \quad (2.9)$$

The non-singular term R_f in eq. (2.1) can be written as

$$R_f(p_T) = \frac{d\sigma_{ZJ}^{(NLO)}}{d\Phi_Z dp_T} - \frac{\alpha_s(p_T)}{2\pi} \left[\frac{d\sigma^{\text{sing}}}{d\Phi_Z dp_T} \right]^{(1)} - \left(\frac{\alpha_s(p_T)}{2\pi} \right)^2 \left[\frac{d\sigma^{\text{sing}}}{d\Phi_Z dp_T} \right]^{(2)}, \quad (2.10)$$

where

$$\frac{d\sigma_{ZJ}^{(NLO)}}{d\Phi_Z dp_T} = \frac{\alpha_s(p_T)}{2\pi} \left[\frac{d\sigma_{ZJ}}{d\Phi_Z dp_T} \right]^{(1)} + \left(\frac{\alpha_s(p_T)}{2\pi} \right)^2 \left[\frac{d\sigma_{ZJ}}{d\Phi_Z dp_T} \right]^{(2)} \quad (2.11)$$

is the differential cross-section at fixed NLO accuracy for $Z + 1$ jet production. In writing these expressions, we are using the notation $[X]^{(i)}$ to denote the i -th component of the expansion of X in powers of $\alpha_s/2\pi$.

The implementation of the MiNLO formula in eq. (2.3) is then given by

$$\begin{aligned} \frac{d\sigma}{d\Phi_Z dp_T} &= \exp[-\tilde{S}(p_T)] \left\{ \frac{\alpha_s(p_T)}{2\pi} \left[\frac{d\sigma_{ZJ}}{d\Phi_Z dp_T} \right]^{(1)} \left(1 + \frac{\alpha_s(p_T)}{2\pi} [\tilde{S}(p_T)]^{(1)} \right) \right. \\ &\quad \left. + \left(\frac{\alpha_s(p_T)}{2\pi} \right)^2 \left[\frac{d\sigma_{ZJ}}{d\Phi_Z dp_T} \right]^{(2)} \right\} \\ &\equiv \frac{d\sigma^{\text{PWG}}}{d\Phi_Z dp_T}, \end{aligned} \quad (2.12)$$

and this term corresponds to the MiNLO \tilde{B} function in the POWHEG language [70].

In the following, we also need the expansion in α_s of $D(p_T)$ and of $\mathcal{L}(p_T)$ in eq. (2.4)

$$D(p_T) = \left(\frac{\alpha_s}{2\pi}\right) [D(p_T)]^{(1)} + \left(\frac{\alpha_s}{2\pi}\right)^2 [D(p_T)]^{(2)} + \dots \quad (2.13)$$

$$[D(p_T)]^{(1)} = - \left[\frac{d\tilde{S}(p_T)}{dp_T} \right]^{(1)} [\mathcal{L}(p_T)]^{(0)} + \left[\frac{d\mathcal{L}(p_T)}{dp_T} \right]^{(1)}, \quad (2.14)$$

$$[D(p_T)]^{(2)} = - \left[\frac{d\tilde{S}(p_T)}{dp_T} \right]^{(2)} [\mathcal{L}(p_T)]^{(0)} - \left[\frac{d\tilde{S}(p_T)}{dp_T} \right]^{(1)} [\mathcal{L}(p_T)]^{(1)} + \left[\frac{d\mathcal{L}(p_T)}{dp_T} \right]^{(2)}, \quad (2.15)$$

where

$$[\mathcal{L}(p_T)]^{(0)} = \sum_{ij} \frac{d|M^Z|_{ij}^2}{d\Phi_Z} f_i^{[a]} f_j^{[b]}, \quad (2.16)$$

$$\begin{aligned} [\mathcal{L}(p_T)]^{(1)} = \sum_{ij} \frac{d|M^Z|_{ij}^2}{d\Phi_Z} & \left\{ H f_i^{[a]} f_j^{[b]} + (C_{iq} \otimes f_q)^{[a]} f_j^{[b]} + (C_{ig} \otimes f_g)^{[a]} f_j^{[b]} \right. \\ & \left. + f_i^{[a]} (C_{jq} \otimes f_q)^{[b]} + f_i^{[a]} (C_{jg} \otimes f_g)^{[b]} \right\}. \quad (2.17) \end{aligned}$$

Here M^Z is the Born matrix element for the Drell-Yan production of the Z boson, $[a]$ and $[b]$ label the incoming partons, i and j stand for the quark flavors in the $q\bar{q} \rightarrow Z$ process, $f_{(q/g)}^{[a/b]}$ are the PDFs, while $C_{k\ell}(z)$ are the hard-collinear functions up to $\mathcal{O}(\alpha_s)$

$$C_{k\ell}(z) = -\hat{P}_{k\ell}^\epsilon(z) - \frac{\pi^2}{12} C_F \delta_{k\ell} \delta(1-z), \quad (2.18)$$

where $\hat{P}_{k\ell}^\epsilon(z)$ is the $\mathcal{O}(\epsilon)$ part of the LO regularized Altarelli-Parisi splitting functions $\hat{P}_{k\ell}(z)$

$$\begin{aligned} \hat{P}_{qq}^{(0)}(z) &= C_F \left[\frac{1+z^2}{(1-z)_+} + \frac{3}{2} \delta(1-z) \right], & \hat{P}_{qq}^\epsilon(z) &= -C_F(1-z), \\ \hat{P}_{qg}^{(0)}(z) &= T_F \left[z^2 + (1-z)^2 \right], & \hat{P}_{qg}^\epsilon(z) &= -2 T_F z(1-z), \end{aligned} \quad (2.19)$$

and we have used the notation

$$(f \otimes g)(x) = \int_x^1 \frac{dz}{z} f(z) g\left(\frac{x}{z}\right). \quad (2.20)$$

The symbol $(\dots)_+$ denotes the usual plus prescription. Equations (2.16) and (2.17) depend explicitly of the phase space of the LO Drell-Yan process, while the dependence on p_T is introduced via the PDF factorization scale choice $\mu_F = p_T$.

3 The MiNLO formalism for QED

In this work, we want to extend the MiNLO method applied up to now to deal with NLO QCD corrections, to NLO QED, in the simplest process, i.e. $pp \rightarrow Z\mathcal{A}$, where \mathcal{A} represents any radiation allowed in QED from the underlying inclusive process ($pp \rightarrow Z \rightarrow \nu\bar{\nu}$), namely: $\mathcal{A}, p = \{q, \bar{q}, \gamma\}$. Specifically, this implies that we neither fix the flavor of the particle produced in association with the Z boson, nor do we require an isolated photon. Instead, we address Z +jet-type processes using a QED analogue of a jet. For the same reasons, the particles in the initial state can be quarks or photons.

Since we are following, as closely as possible, the QCD MiNLO formulation for F +jet production, with F colorless, in order to apply it to the QED case, we limit ourselves to considering Z decay into neutrinos, to prevent final-state radiation (FSR) emissions from the decay products. The inclusion of FSR from leptons could be obtained by following the MiNLO formulation for the $t\bar{t}$ +jet process described in Refs. [105, 112], provided that massive leptons are considered. This is left to future developments.

Adhering closely to the original QCD MiNLO formalism also requires addressing two additional aspects specific to the QED case: the running of the electromagnetic coupling constant and the replacement of the color factors with their QED counterparts. Both aspects play a crucial role in determining the position of the Sudakov peak in QED, and we discuss them in the following.

3.1 The running of the electromagnetic coupling

In the evaluation of the Feynann diagrams, the coupling constant at the vertexes of the Z -boson propagator with the initial-state hadronic current and with the final-state neutrinos can be assumed as independent from the coupling used by MiNLO when generating radiation. For this reason, even if these couplings can be written in terms of the electric charge, and ultimately in terms of the electromagnetic coupling, they can be fixed at a constant value of α , independently of the value of α used for the radiation, typically running.

As far as the generation of QED radiation is concerned (i.e. the $q\bar{q}\gamma$ vertexes), in the MiNLO formulae we have to substitute $\alpha_s(\mu)$ with the electromagnetic running coupling $\alpha(\mu)$ defined in the $\overline{\text{MS}}$ scheme. Indeed, the original MiNLO prescription requires that the ISR splitting coupling that appears in the tree-level process $pp \rightarrow Z\mathcal{A}$ is evaluated in the $\overline{\text{MS}}$ scheme at the scale p_T . This same choice is consistently adopted for both the NLO real and virtual corrections. After renormalization, the $q\bar{q}\gamma$ vertex develops a contribution of the form

$$\alpha(\mu) (1 + 2\delta Z_e(\mu) + \delta Z_\gamma) \quad (3.1)$$

where $\delta Z_e(\mu)$ is the electric charge counterterm in the $\overline{\text{MS}}$ scheme at the renormalization scale μ , while δZ_γ is the $\mathcal{O}(\alpha)$ component of the Lehmann–Symanzik–Zimmermann factor for the external photon.

In this paper we are interested in keeping an arbitrary scale μ in the running of the electromagnetic coupling constant α , without resorting to α_0 , the Thompson value of the electromagnetic coupling. The contribution in eq. (3.1) then develops large corrections associated with the fermionic loops (see e.g. [113]). In fact, if the fermions are treated as massive, then large logarithms of the fermion masses appear. If they are treated as massless, then the expression is affected by the presence of infrared poles. The correct treatment of these poles implies that we have also to include, in the real corrections, diagrams of the type $q\bar{q} \rightarrow Zq'\bar{q}'$ plus all their crossings.⁶

In this paper we are considering a simplified case study, where only u and d quarks are present, and the PDFs evolve only via QED. The running of α is then performed at two loops in QED, with the sole contributions of up and down quarks. The running is frozen below an arbitrary cutoff (of the order of the electron mass), where α is set equal to $\bar{\alpha}_0$.

Unless stated otherwise, in the following we will use $\bar{\alpha}_0 = 0.04$ as the starting value for the running of α , corresponding to approximately five times its physical value. The rationale for this choice is that, in investigating the application of MiNLO to QED, we aim to analyze effects proportional to the electromagnetic coupling. An enhanced coupling magnifies these QED effects, allowing us to obtain statistically significant corrections with a moderate computational cost in the Monte Carlo simulations. Nonetheless, the chosen value of $\bar{\alpha}_0$ remains sufficiently small to keep the running of α moderate over the entire range of scales probed by our setup, ensuring that the qualitative behavior of the QED corrections is not drastically altered.

In a more realistic context where QED corrections are calculated alongside QCD corrections, one could use the Standard Model running of α (following, for instance, Ref. [116]), taking $\alpha(M_Z)$ in the $\overline{\text{MS}}$ scheme as input and then evolving it to low scales down to the minimum value of p_T used for the calculation (of the order of a GeV), thereby reducing the dependence of the running on the light degrees of freedom (as done in Refs. [117, 118]). The possibility of reformulating MiNLO without using the $\overline{\text{MS}}$ scheme for the QED coupling is left for future exploration.

3.2 The color factors

The coefficients $A^{(i)}$ and $B^{(i)}$ in eq. (2.8), as well as the hard-virtual function H in eq. (2.9), the collinear coefficient functions in eq. (2.18) and the corresponding

⁶We have implemented the corresponding FKS [114, 115] subtraction terms and their integrated counterparts in the `POWHEG BOX RES`, in order to deal with these QED singularities.

splitting functions in eq. (2.19), must be abelianized, with the following replacements

$$C_A \rightarrow 0, \quad C_F \rightarrow Q_f^2, \quad T_F \rightarrow N_c^f Q_f^2, \quad \beta_0 \rightarrow \beta_0^{\text{QED}}, \quad (3.2)$$

where Q_f is the fermionic electric charge. Here, β_0^{QED} is related to the running of $\alpha(\mu)$ in the $\overline{\text{MS}}$: since we will limit ourselves for simplicity to a simplified parton model involving only up and down quarks, we have

$$\beta_0^{\text{QED}} = -\frac{(Q_u^2 + Q_d^2)}{\pi}. \quad (3.3)$$

3.3 The QED Sudakov peak and the implications for the MiNLO formulation

The most striking difference with respect to QCD turns out to be the position of the Sudakov peak. From the expression for the Z boson transverse-momentum distribution in eqs. (2.1) and (2.2), by observing that the most singular contributions in the limit $p_T \rightarrow 0$ are associated with the derivative of \tilde{S} (which generates terms of the form $1/p_T \log(Q^2/p_T^2)$) as can be seen in eq. (2.6), it is possible to estimate the position of the peak in the p_T spectrum by finding the maximum of $d[e^{-\tilde{S}(p_T)}]/dp_T$. In QCD, this procedure leads to estimating the spectrum peak from a few GeV to tens of GeV, depending on the colorless system produced. In QED the peak position is several orders of magnitude lower and well outside the practically accessible region. In fact, one can easily see that, for α fixed (and this is a very good approximation in QED), the position of the peak is approximately given by

$$p_T^{\text{peak}} = Q \exp\left(-\frac{\pi}{4Q_f^2 \alpha}\right). \quad (3.4)$$

For example, for an up-type quark ($Q_f = 2/3$), with $Q = M_Z$ and $\alpha = \alpha_0 \equiv 1/137$ we get $p_T^{\text{peak}} \approx 6.5 \times 10^{-104}$ GeV. This fact mainly arises from the different behavior of the coupling constant at small p_T : in QCD, $\alpha_s(p_T)$ is divergent when $p_T \rightarrow 0$, while in QED $\alpha(p_T)$ tends to α_0 . In addition to this, the numerical values of the QCD and QED couplings that appear in the exponential have an important impact too, together with the differences among the values of the coefficients $A^{(i)}$ and $B^{(i)}$ in the two theories.

The position of the Sudakov peak is crucial: in fact, as it stands, eq. (2.1) is such that its integral over p_T , between an infrared cutoff Λ (more precisely, the scale value where the Sudakov form factor in eq. (2.2) vanishes) and Q , reproduces the NLO inclusive cross section for Z production. While not conceptually problematic, its position is so low that any numerical evaluation of the actual implementation of the MiNLO formula, i.e. eq. (2.12), is unfeasible, since the Born, the real and the virtual

amplitudes entering this equation will be unstable and unreliable when evaluated for such low values of the transverse momentum.⁷

In order to circumvent this obstacle, we have adopted the following strategy: the p_T spectrum in eq. (2.1) is divided into two regions, below and above a technical cutoff p_T^c ,

$$\frac{d\sigma}{d\Phi_z dp_T} = \frac{d\sigma^<}{d\Phi_z dp_T} + \frac{d\sigma^>}{d\Phi_z dp_T}, \quad (3.5)$$

where, according to eqs. (2.2) and (2.12),

$$\frac{d\sigma^<}{d\Phi_z dp_T} \equiv \frac{d}{dp_T} \left\{ \exp[-\tilde{S}(p_T)] \mathcal{L}(p_T) \right\} + R_f(p_T) \quad \text{for } p_T < p_T^c, \quad (3.6)$$

$$\frac{d\sigma^>}{d\Phi_z dp_T} \equiv \frac{d\sigma^{\text{PWG}}}{d\Phi_z dp_T} \quad \text{for } p_T > p_T^c. \quad (3.7)$$

In the region above p_T^c , the original MiNLO method, appropriately abelianized, is applied.

Recalling that the $R_f(p_T)$ term is non singular in the $p_T \rightarrow 0$ limit, we expect this term to behave as power corrections in p_T . In the region below p_T^c , we then assume that the regular terms $R_f(p_T)$ in eq. (3.6) can be neglected, and the differential cross section can be expressed as an exact differential in p_T . We can then integrate over the Z boson transverse momentum (that is nevertheless assumed as small, since we are in the region $p_T < p_T^c$) and obtain

$$\frac{d\sigma^<}{d\Phi_z} = \exp[-\tilde{S}(p_T^c)] \left\{ [\mathcal{L}(p_T^c)]^{(0)} + \frac{\alpha(p_T^c)}{2\pi} [\mathcal{L}(p_T^c)]^{(1)} \right\}, \quad (3.8)$$

where we have expanded the luminosity $\mathcal{L}(p_T^c)$ in series of α , using the abelianization of eqs. (2.16) and (2.17). In this way, the kinematics of the events in the region $p_T < p_T^c$ is correctly computed according to the expression in eq. (3.8), and the NLO accuracy in the totally inclusive Z boson production is reached.

The validity of having disregarded the non-singular term $R_f(p_T)$ in this region will be discussed in Sec. 5.

3.4 The QED evolution of parton distribution functions

Since we are considering the MiNLO QED corrections to $pp \rightarrow Z\mathcal{A}$ production, we would need a PDF set evolved only with QED kernels. This is due to fact that there is an interplay between the factorization scale μ_F , used for the PDF calculation, and the terms in the MiNLO formulae, that evolve the PDFs from the initial scale μ_F , of the order of p_T , up to the hard process scale, i.e. the virtuality of the Z boson.

⁷These considerations are even more relevant when combining the QED and QCD corrections, since, in this case, the choice of the infrared cutoff Λ would be constrained by the condition that QCD remains in its perturbative regime and Λ should not go below $\mathcal{O}(1)$ GeV.

If we were to use PDFs containing also QCD evolution effects without including QCD corrections in the MiNLO formula, the residual scale dependence would be large and would correspond to the one of a leading-order calculation (in QCD).

Since in this paper we are only interested in presenting the QED MiNLO formalism as a case study, we have built an ad-hoc PDF set, that we evolve only with QED kernels, from very low scales up to the Z mass. We proceeded as follows: we used the latest version of the HOPPET library [119, 120], which allows to evolve a PDF set, starting from a grid defined at a given reference scale, performing only the QED evolution. To date, the QED evolution has been performed only at leading order. The consequences of this will be further discussed in Sec. 5. In addition, we have modified the HOPPET library to eliminate the QCD evolution and to lower the minimum μ_F value achievable in the evolution. The running of α was also modified to match exactly what described in Sec. 3.1.

The way we have obtained this ad-hoc PDF has a very large degree of arbitrariness. Our goal was only to have a set with the quarks and photon PDFs of comparable size, to put on the same footing diagrams initiated only by quarks and those where a photon is present in the initial state. In particular, for the numerical analysis presented in this work, we started with the `NNPDF31_nlo_as_0118_luxqed` set [121–123], at its minimum q value (1.65 GeV), and we have used this set as input to the QED-only evolution supplied by HOPPET, where we have set the starting scale for the evolution to be 0.01 GeV.

Since the PDFs obtained in this way exhibit a sort of transient at small evolution scales (where the photon PDF grows very rapidly at the expense of the quarks), we reiterated the above procedure by using this set to obtain a new initial condition for the evolution (computed where we have an equilibrium between the quarks and the photon content), and repeated the evolution starting from $q = 0.01$ GeV. The PDFs of the resulting set, although they grow quite rapidly between 0.01 and $\mathcal{O}(1)$ GeV, no longer show important relative variations between the different quark flavors and the photon.

4 Implementation of the QED MiNLO formulae

The calculation of the NLO QED corrections to the process $pp \rightarrow Z\mathcal{A}$ has been implemented within the `POWHEG BOX RES` [72] framework and utilizes external libraries such as LHAPDF [124] and HOPPET [119, 120] for PDF management (see Sec. 3.4) and RECOLA [125–129] for the computation of tree-level and one-loop matrix elements.

It is important to note that, since the strategy of our study is to follow the original MiNLO implementation for QCD as closely as possible, quarks and photons are treated exactly on equal footing in our calculation. This specifically implies that the calculation includes the tree-level and virtual matrix elements for all processes

of the type $q\bar{q} \rightarrow Z\gamma$ and $\gamma q(\bar{q}) \rightarrow Zq(\bar{q})$, while the real contributions consist of the processes $q\bar{q} \rightarrow Z\gamma\gamma$, $\gamma q(\bar{q}) \rightarrow Zq(\bar{q})\gamma$, $\gamma\gamma \rightarrow Zq\bar{q}$ and $q\bar{q} \rightarrow Zq'\bar{q}'$, plus crossings, with q equal or different from q' (see also the discussion in Sec. 3.1). In our case study, we limit ourselves to a simplified theory in which only up and down quarks are present.

We have computed analytically the virtual photonic corrections for the $pp \rightarrow Z\mathcal{A}$ process. The rationale behind this is that we want a code that is perfectly stable also in the singular regions. Indeed, we have also computed analytically the soft and collinear limits of the virtual amplitudes, as Taylor expansion of the full analytic result, greatly increasing the precision and numerical stability in the small p_T limit, if compared to any numerical calculation of the virtual amplitudes.

To check the calculation we have also computed the virtual corrections with RECOLA, using its interface implemented in the **POWHEG BOX RES** code, and found very good agreement in kinematic configurations where the transverse momentum of the Z boson is sufficiently large to be away from any singular region.

In the class of the virtual corrections, we have to consider also the fermionic loops that enter in the counterterm of $\alpha(\mu)$ and in the δZ_γ factor (in the notation of Refs. [6, 130]) associated with the external photon, and are added a posteriori to the virtual corrections, being proportional to the Born amplitude.

To verify that the QED MiNLO code reaches the NLO accuracy for the fully inclusive process $pp \rightarrow Z$, we compared the MiNLO results both to a dedicated code, implemented in the **POWHEG BOX RES** framework, and to a modified version of the public **Z_ew-BMNNPV** code.⁸

The electroweak parameters are computed in a hybrid scheme where the input parameters are $\alpha(\mu)$ in the $\overline{\text{MS}}$ scheme, M_W and M_Z .

5 Validation and results

The goal of this section is to study how well the QED MiNLO formalism, based on a calculation that has NLO QED accuracy for the process $pp \rightarrow Z\mathcal{A}$, approaches the NLO accuracy for the process $pp \rightarrow Z$, when fully inclusive quantities are computed, and to validate some of the approximations that we have discussed in Sec. 3.

For this reason, we present a few numerical results obtained with the main purpose of verifying the internal consistency of the MiNLO method we have implemented and to quantify the degree of approximation it has. It is important to emphasize from the outset that, due to the choice made for the value of α , in Sec. 3.1, and of the PDFs set that we have used, in Sec. 3.4, the absolute predictions for the cross

⁸The modified version of the code now includes processes where the Z decays into neutrinos. In addition, also the γ -induced processes were added. The implementation details and phenomenological impact of these diagrams on the Drell-Yan precision physics will be documented in a dedicated publication.

sections and distributions, as well as the relative NLO versus LO corrections, are not realistic: these choices were made just to amplify the effect of the QED corrections, so that to highlight any possible problem in the formalism. The conclusions we draw, regarding the agreement between the MiNLO results and the corresponding ones for the totally inclusive Z production, remain valid for the actual value of the physical parameters.

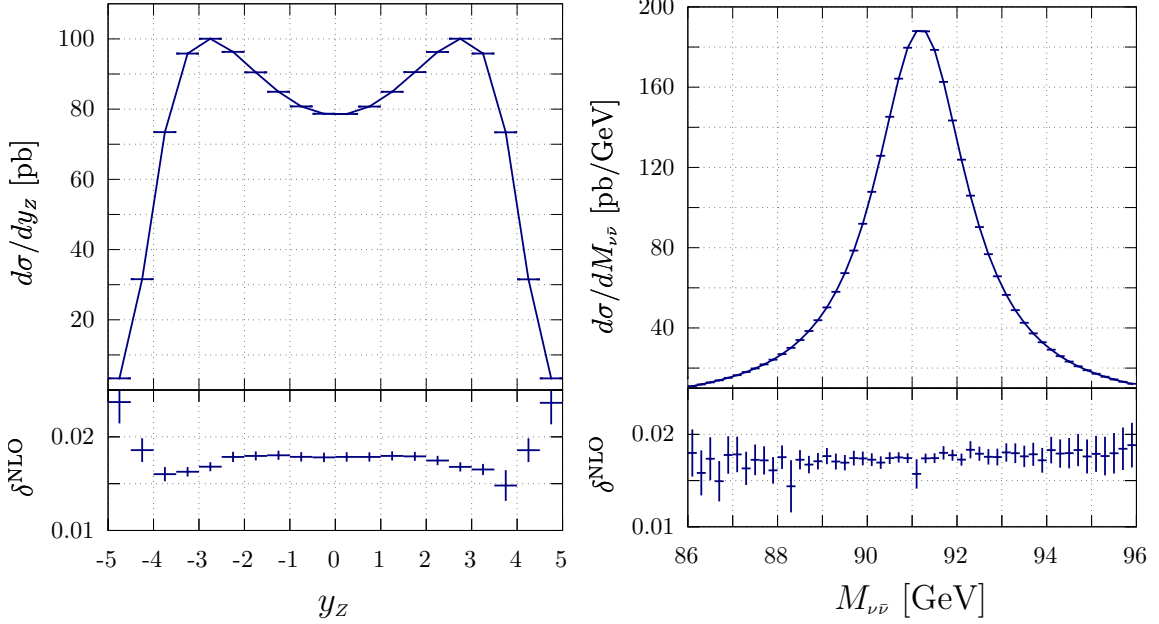


Figure 1. Differential distributions for the inclusive process $pp \rightarrow Z$ as a function of the neutrino pair rapidity (left) and invariant mass (right) at NLO. The lower panels show the ratio of the NLO over the LO corrections, with $\mu_F = M_Z$. The value of α entering the corrections corresponds to $\alpha(\mu_R = M_Z)$, evolved from $\alpha(0) = \bar{\alpha}_0 = 0.04$. The PDF choice is detailed in Sect. 3.4. The γ -induced contributions enter the calculation at NLO.

The first thing to assess is the size of the NLO corrections with respect to the LO, for the fully inclusive process, i.e. Z boson production in Drell-Yan, with the Z decaying into neutrinos. In Fig. 1 we plot the rapidity and the invariant mass of the neutrino pair, and δ^{NLO} is the ratio between the NLO over the LO differential cross section. The plots show that the effects are positive and of the order of 2%. The corrections are flat across the ranges used in the figures, although, at large absolute rapidities, the corrections tend to increase. It should be noted that the power of α connected with the photonic radiation for the inclusive Drell-Yan is evaluated in the $\overline{\text{MS}}$ scheme, at the scale $\mu_R = M_Z$, as described in Sec. 3.1.

In order to estimate the effect of having neglected the finite contribution R_f in the region below p_T^c in eq. (3.6), we have compared the expansion of the MiNLO formulae at first order in α , in both the regions, below (see eq. (3.8)) and above (see eq. (3.7))

M_Z/p_T^c	$\sigma_{\mathcal{O}(\alpha)}^>$	$\sigma_{\mathcal{O}(\alpha)}^<$	$\sigma_{\mathcal{O}(\alpha)}^> + \sigma_{\mathcal{O}(\alpha)}^<$	$\sigma_{\text{NLO}}^{\text{DY}}$	$\sigma_{\text{LO}}^{\text{DY}}$	δ_α
1	2.0191(5)	730.4(1)	732.5(1)	735.346(7)	722.818(4)	-0.0039(2)
5	20.353(5)	714.7(1)	735.0(1)	734.859(7)	708.472(4)	0.0003(2)
10	36.35(1)	698.3(1)	734.7(1)	734.437(5)	702.774(4)	0.0003(2)
20	57.57(2)	676.4(1)	734.0(1)	733.63(1)	697.359(4)	0.0005(3)
50	93.456(3)	639.3(1)	732.7(1)	732.476(7)	690.638(4)	0.0004(2)
100	126.181(4)	605.1(1)	731.3(1)	731.24(1)	685.897(4)	0.0001(2)
200	163.566(5)	565.9(1)	729.5(1)	729.395(5)	681.490(4)	0.0001(2)

Table 1. Integrated cross sections, in pb, obtained with the $\mathcal{O}(\alpha)$ expansion of the MiNLO formulae for the regions below ($\sigma_{\mathcal{O}(\alpha)}^<$) and above ($\sigma_{\mathcal{O}(\alpha)}^>$) p_T^c , for some values of the technical cut ranging from M_Z to $M_Z/200$. The factorization scale μ_F in both the MiNLO and the target predictions is always set to p_T^c , while the power of the radiation α is set to $\alpha(\mu = M_Z)$. The sum of the cross sections above and below p_T^c is compared to the cross section for the target process $pp \rightarrow Z$ at NLO. The last column shows the relative difference between the MiNLO prediction expanded at order $\mathcal{O}(\alpha)$ and $\sigma_{\text{NLO}}^{\text{DY}}$, as defined in eq. (5.1).

the technical cut p_T^c , and we have compared their sum to the fixed-order prediction for Drell-Yan at NLO accuracy. The differences between these two contributions gives the size of the neglected term R_f . In Table 1, we then present the total cross sections obtained with the expanded MiNLO formulae, both in the regions below, $\sigma_{\mathcal{O}(\alpha)}^<$, and above, $\sigma_{\mathcal{O}(\alpha)}^>$, the technical cut p_T^c . Their sum is compared with the prediction for Drell-Yan at NLO accuracy (the results obtained for Drell-Yan at LO are also reported for completeness). In the last column we report the value of

$$\delta_\alpha \equiv \frac{\sigma_{\mathcal{O}(\alpha)}^> + \sigma_{\mathcal{O}(\alpha)}^<}{\sigma_{\text{NLO}}^{\text{DY}}} - 1. \quad (5.1)$$

According to the discussion in Sec. 3.1, the radiation α in all the cross sections in Table 1 is computed in the $\overline{\text{MS}}$ scheme at $\mu_R = M_Z$. We note that any variations of this scale in the predictions obtained with MiNLO in the above and below p_T^c regions would, in any case, be of order $\mathcal{O}(\alpha^2)$. The cross sections for the p_T spectrum region above p_T^c is the LO contribution to $pp \rightarrow Z\mathcal{A}$, while, for the region below p_T^c , according to eq. (3.8), the $\mathcal{L}^{(0)}$ and $\mathcal{L}^{(1)}$ expansion of the luminosity in eqs. (2.16) and (2.17) appear, along with the $\mathcal{O}(\alpha)$ expansion of the Sudakov form factor. In the calculation of these cross sections, the PDFs are evaluated at $\mu_F = p_T^c$.

From Table 1, it can be observed that, for all considered values of p_T^c except M_Z , the MiNLO formula expanded to $\mathcal{O}(\alpha)$ is in agreement with the inclusive NLO target, within the numerical error. This allows us to conclude that the $\mathcal{O}(\alpha)$ regular term R_f , in the region below p_T^c is negligible, and it is reasonable to assume that the $\mathcal{O}(\alpha^2)$ terms are negligible too. This supports the procedure discussed in Sec. 3.

The table also shows the dependence of the total cross sections on the factorization scale μ_F : the effect of varying μ_F , while being considerably reduced in the transition from LO to NLO, becomes progressively more pronounced as p_T^c decreases. This is a consequence of the PDFs we have adopted, whose μ_F dependence is rather steep in the region below the GeV.

M_Z/p_T^c	$\sigma^>$	$\sigma_{\text{LO}}^>$	$\sigma^<$	$\sigma^> + \sigma^<$	$\delta_{\text{MiNLO}}^{\text{FO}}$	$\delta_{\text{MiLO}}^{\text{FO}}$
1	2.249(2)	2.018(2)	730.18(4)	732.43(4)	-0.0039(1)	-0.00427(5)
5	21.80(1)	20.60(1)	714.39(4)	736.19(4)	0.0011(1)	-0.00047(5)
10	38.27(2)	36.48(1)	698.46(4)	736.73(4)	0.0019(1)	-0.00054(5)
20	59.30(3)	56.96(2)	677.82(3)	737.13(5)	0.0024(1)	-0.00077(5)
50	93.13(4)	90.02(3)	644.52(3)	737.66(5)	0.0031(1)	-0.00102(6)
100	122.29(6)	118.60(3)	615.77(3)	738.07(6)	0.0037(1)	-0.00131(6)
200	153.58(8)	149.33(4)	584.86(3)	738.45(8)	0.0042(2)	-0.00156(7)

Table 2. MiNLO predictions for the integrated cross sections, in pb, below ($\sigma^<$) and above ($\sigma^>$ and $\sigma_{\text{LO}}^>$) the separator p_T^c , for some values of the technical cut ranging from M_Z to $M_Z/200$. The cross section $\sigma_{\text{LO}}^>$ represents the integrated cross section above p_T^c , computed with the MiNLO and MiLO methods (see the text for more details). The last two columns show the relative difference between $\sigma^< + \sigma^>$ ($\sigma^< + \sigma_{\text{LO}}^>$) and the (inclusive) total cross section for the reference process $pp \rightarrow Z$ at NLO. In this case, the target process is computed for $\mu_F = M_Z$ and its total cross section is given in eq. (5.2).

In Table 2 we collect the value of the cross sections computed with the MiNLO method, in the region below and above p_T^c , their sum, and the relative difference between the MiNLO predictions and the reference target. Note that the target now is the NLO Drell-Yan cross section, computed with $\mu_F = M_Z$, and with the electromagnetic coupling $\alpha(\mu_R)$ computed in the $\overline{\text{MS}}$ scheme with $\mu_R = M_Z$. The reason for this choice of scales is that the MiNLO formulae effectively perform the evolution of the contributions evaluated at the scale $\mu_F = \mu_R = p_T$ up to the hard scale of the inclusive reference process (in this case, M_Z). The target cross section is $\sigma_{\text{NLO}}^{\text{DY}}$ in Table 1, in the first line, i.e.

$$\sigma_{\text{ref}} = 735.346 \pm 0.007 \text{ pb}. \quad (5.2)$$

The relative difference between the MiNLO predictions and the reference target is then defined as

$$\delta_{\text{MiNLO}}^{\text{FO}} = \frac{\sigma^> + \sigma^<}{\sigma_{\text{ref}}} - 1. \quad (5.3)$$

Table 2 also shows a second set of results, where the cross section above p_T^c is computed in a LO variant of the MiNLO method, that we dub MiLO. Referring to eq. (2.12), in the MiLO version, only the Born contribution to the $pp \rightarrow Z\mathcal{A}$ process

contributes in the curly brackets, and the Sudakov form factor in front is evaluated including only the A_1 and B_1 terms in eq. (2.7).

In order to better interpret the numerical results, it might be useful to recall the expression for the singular part of the cross section $d\sigma^{\text{sing}}$ in eq. (2.2) in the MiNLO method [101], written as in eq. (2.3),

$$\frac{d\sigma^{\text{sing}}}{d\Phi_Z dp_T} = e^{-\tilde{S}(p_T)} \frac{d|M^Z|_{ij}^2}{d\Phi_Z} \frac{2}{p_T} \sum_{n=1}^2 \sum_{m=0}^1 \left(\frac{\alpha(p_T)}{2\pi} \right)^n {}_n E_m \log^m \left(\frac{Q^2}{p_T^2} \right), \quad (5.4)$$

where the coefficients ${}_n E_m$, using the same notation as in eqs. (2.16) and (2.17), read

$$\begin{aligned} {}_1 E_1 &= A^{(1)} f_i^{[a]} f_j^{[b]}, \\ {}_1 E_0 &= B^{(1)} f_i^{[a]} f_j^{[b]} + (P_{ik}^{(0)} \otimes f_k)^{[a]} f_j^{[b]} + f_i^{[a]} (P_{jk}^{(0)} \otimes f_k)^{[b]}, \\ {}_2 E_1 &= \frac{1}{2} A^{(2)} f_i^{[a]} f_j^{[b]} + A^{(1)} \left[\frac{1}{2} H f_i^{[a]} f_j^{[b]} + (C_{ik} \otimes f_k)^{[a]} f_j^{[b]} \right] + \{i \leftrightarrow j\}, \\ {}_2 E_0 &= \frac{1}{2} \tilde{B}^{(2)} f_i^{[a]} f_j^{[b]} + (B^{(1)} - 2\pi\beta_0^{\text{QED}}) \left[\frac{1}{2} H f_i^{[a]} f_j^{[b]} + (C_{ik} \otimes f_k)^{[a]} f_j^{[b]} \right] \\ &\quad + H (P_{ik}^{(0)} \otimes f_k)^{[a]} f_j^{[b]} + (C_{ik} \otimes P_{kl}^{(0)} \otimes f_l)^{[a]} f_j^{[b]} + (C_{ik} \otimes f_k)^{[a]} (P_{jl}^{(0)} \otimes f_l)^{[b]} \\ &\quad + (P_{ik}^{(1)} \otimes f_k)^{[a]} f_j^{[b]} + \{i \leftrightarrow j\}. \end{aligned} \quad (5.5)$$

The terms ${}_1 E_1$ and ${}_1 E_0$ represent the Born-level contribution to the process $pp \rightarrow Z\mathcal{A}$ and correspond to the $\mathcal{O}(\alpha)$ contribution of $d\{\exp[-\tilde{S}(p_T)]\mathcal{L}(p_T)\}/dp_T$ in eq. (2.2). So, as long as we restrict ourselves to the singular part of the cross section, MiLO corresponds to eq. (5.4), where the Sudakov form factor contains only $\mathcal{O}(\alpha)$ terms and where only the terms ${}_1 E_1$ and ${}_1 E_0$ are non vanishing. The terms ${}_2 E_1$ and ${}_2 E_0$ are the singular limit of the real and virtual corrections to $pp \rightarrow Z\mathcal{A}$, from which the first-order expansion of the exponential in eq. (5.4) has been subtracted. This subtraction is necessary to eliminate the $\log^3(Q^2/p_T^2)$ and $\log^2(Q^2/p_T^2)$ terms, otherwise present in the expression of the Z boson p_T spectrum at NLO [131].

To interpret the results for $\delta_{\text{MiNLO}}^{\text{FO}}$ in Table 2, we need to consider also the following issues:

1. The cancellation of the $\log^m(Q^2/p_T^2)$ ($m = 2, 3$) terms is purely numerical in MiNLO and can become critical when studying relative differences at the per mille level (as in this case).
2. The terms containing the one-loop corrections to the Altarelli-Parisi kernels, $P_{ij}^{(1)}$ in eq. (5.5), arise from the collinear limit of the double-radiation contributions and should correspond to the $\mathcal{O}(\alpha^2)$ component of the PDF evolution equation. The HOPPET code we have used does not provide QED evolution of the PDFs at this order. So the PDF evolution does not include $\mathcal{O}(\alpha)$ corrections to the Altarelli-Parisi kernels, and the expression in eq. (5.4) is no

longer exactly equal to the derivative of $\exp[-\tilde{S}(p_T)]\mathcal{L}(p_T)$ with respect to p_T of eq. (2.2). This gives rise to a mismatch in the sum of the cross sections $\sigma^>$ and $\sigma^<$ that depends on the p_T^c cutoff.

3. In addition to terms singular in the $p_T \rightarrow 0$ limit, the MiNLO cross section contains also regular contributions of order α and α^2 (the R_f term). The contribution at order α is necessary to reproduce the NLO corrections to the totally inclusive Drell-Yan process $pp \rightarrow Z$. The contribution at order α^2 is necessary to reproduce the NLO corrections for $pp \rightarrow Z\mathcal{A}$. But when comparing MiNLO and the target cross section, this contribution is effectively a spurious higher-order effect, that can contribute to give some discrepancies between MiNLO and the target.

On the other hand, the MiLO results are not affected by the aforementioned issues. However, they contain neither the $\mathcal{O}(\alpha^2)$ term associated with the derivative of the Sudakov form factor (see the first term in eq. (2.15)), nor the terms related to $\alpha(p_T)[\mathcal{L}(p_T)]^{(1)}$ and its derivative with respect to p_T , which are nevertheless necessary to achieve NLO accuracy for observables inclusive in the Z boson transverse momentum. The former contribution consists in the $A^{(2)}$ and $\tilde{B}^{(2)}$ terms of the ${}_2E_1$ and ${}_2E_0$ coefficients in eq. (5.5) and it can be written as the difference

$$\Delta = \frac{d}{dp_T} \left\{ \exp \left[-\tilde{S}(p_T) \right] [\mathcal{L}(p_T)]^{(0)} \right\} - \frac{d}{dp_T} \left\{ \exp \left[-\tilde{S}_1(p_T) \right] [\mathcal{L}(p_T)]^{(0)} \right\}, \quad (5.6)$$

where \tilde{S}_1 is a short-hand notation for \tilde{S} , computed including only the $A^{(1)}$ and $B^{(1)}$ coefficients. We can further manipulate Δ to get

$$\begin{aligned} \Delta = -\exp \left[-\tilde{S}(p_T) \right] & \left\{ \left[\frac{d\tilde{S}(p_T)}{dp_T} - \frac{d\tilde{S}_1(p_T)}{dp_T} \exp \left(\tilde{S}(p_T) - \tilde{S}_1(p_T) \right) \right] [\mathcal{L}(p_T)]^{(0)} \right. \\ & \left. + \frac{d}{dp_T} \left([\mathcal{L}(p_T)]^{(0)} \right) \left[1 - \exp \left(\tilde{S}(p_T) - \tilde{S}_1(p_T) \right) \right] \right\}, \end{aligned} \quad (5.7)$$

and, since $\exp \left(\tilde{S}(p_T) - \tilde{S}_1(p_T) \right) = 1 + \mathcal{O}(\alpha^2)$ and $d([\mathcal{L}(p_T)]^{(0)})/dp_T = \mathcal{O}(\alpha)$, using eq. (2.6) for the derivative of the Sudakov form factor, we get

$$\Delta = \exp \left[-\tilde{S}(p_T) \right] \frac{2}{p_T} \left(\frac{\alpha(p_T)}{2\pi} \right)^2 \left\{ A^{(2)} \log \frac{Q^2}{p_T^2} + \tilde{B}^{(2)} \right\} [\mathcal{L}(p_T)]^{(0)} + \mathcal{O}(\alpha^3). \quad (5.8)$$

In a similar way, it can be shown that the remaining terms of ${}_2E_1$ and ${}_2E_0$, omitting the $P_{ik}^{(1)}$ contribution that is missing in the evolution of the PDF set, as discussed in

Sec. 3.4, can be cast in the form⁹

$$\frac{d}{dp_T} \left\{ \exp \left[-\tilde{S}_1(p_T) \right] \frac{\alpha(p_T)}{2\pi} [\mathcal{L}(p_T)]^{(1)} \right\}. \quad (5.10)$$

The missing contributions to the integrated cross-section in the MiLO approximation can thus be estimated analogously to the procedure used for $\sigma^<$ in eq. (3.8), i.e. by integrating the exact differentials in eqs. (5.6) and (5.10), between the technical cutoff p_T^c and the hard process scale.

By including also these contributions in $\sigma_{LO}^>$, the relative discrepancy δ_{MiLO}^{FO} (defined as δ_{MiNLO}^{FO} in eq. (5.3) but with $\sigma^>$ replaced by $\sigma_{LO}^>$), shown in the last column of Table 2, reduces to approximately 0.5 per mille for p_T^c below 20 GeV, confirming the fact that the implementation is correct and the formalism we have proposed is sound.

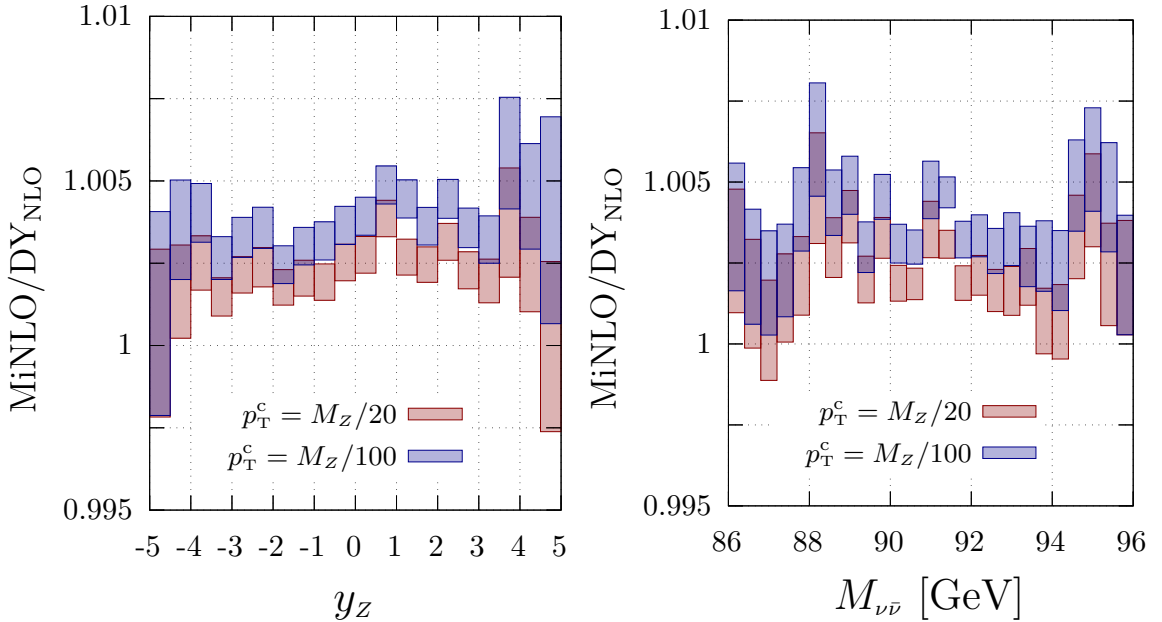


Figure 2. Ratio between the MiNLO predictions for $pp \rightarrow Z\mathcal{A}$ and the target process $pp \rightarrow Z$ at NLO QED as a function of the neutrino pair rapidity (left) and invariant mass (right). The predictions for the Drell-Yan process are the same ones shown in Figure 1, while the MiNLO results correspond to the sum of the contributions above and below p_T^c , for the technical cut equal to $M_Z/20$ and $M_Z/100$.

Turning now to more differential quantities, in Fig. 2 we show the MiNLO differential cross section for the inclusive production of a Z boson, as a function of the

⁹Here we also need to use

$$\frac{d\alpha(p_T)}{dp_T} = -\frac{2}{p_T} \beta_0^{\text{QED}} \alpha^2(p_T) + \mathcal{O}(\alpha^3). \quad (5.9)$$

rapidity and of the invariant mass of the two neutrinos, for two values of the technical cut p_T^c : $M_Z/20$ and $M_Z/100$. Similarly to the conclusions on the total cross sections derived from Table 2, the agreement between the MiNLO differential cross sections and the NLO target is of the order of a few per mille, to be compared to the size of the NLO corrections with respect to the LO one, depicted in Fig. 1, of the order of 2%, for the augmented value of α that we are using in this section.

M_Z/p_T^c	$\sigma^>$	$\sigma^<$	$\sigma^> + \sigma^<$	$\delta_{\text{MiNLO}}^{\text{FO}}$
1	0.1172(1)	651.41(1)	651.53(1)	-0.00249(2)
5	1.5765(4)	651.41(1)	652.99(1)	-0.00026(2)
10	3.245(1)	649.88(1)	653.12(1)	-0.00005(2)
20	5.739(1)	647.44(1)	653.18(1)	0.00004(2)
50	10.360(1)	642.86(1)	653.21(1)	0.00009(2)
100	14.845(2)	638.389(4)	653.235(5)	0.00011(1)
200	20.165(3)	633.090(4)	653.255(5)	0.00015(1)

Table 3. MiNLO predictions for the integrated cross sections, in pb, below ($\sigma^<$) and above ($\sigma^>$) the technical cut p_T^c , ranging from M_Z to $M_Z/200$, and for realistic value of the electromagnetic coupling $\alpha = \bar{\alpha}_0 = 0.008$. In the last column, the relative difference as defined in eq. (5.3), with $\sigma_{\text{ref}} = 653.160(6)$ pb, the total cross section for the reference process $pp \rightarrow Z$ at NLO computed for $\mu_F = M_Z$. In this table, the PDF set used has been consistently evolved with the same choice of the value for α . Note that the LO prediction for the reference process is 650.73(1) pb, so that the relative NLO corrections for $pp \rightarrow Z$ amount to 3.74(2) per mille.

If we use instead the physical value of α , the corrections are reduced by about six times, and this also reduces the difference between the predictions for the target process at NLO and the ones for $Z\mathcal{A}$ production, obtained with MiNLO, as well as the residual p_T^c dependence of the results. This is shown in Table 3, where the calculation of Table 2 has been repeated using an initial value for the running of α equal to $\bar{\alpha}_0 = 0.008$. In this setup, the NLO total cross section for the inclusive Z production turns out to be 653.160(6) pb, and the LO one 650.73(1) pb, so that the NLO corrections reduce to approximately 3.74(2) per mille.

However, the absolute difference (and, to a good approximation, the relative one as well) between the MiNLO predictions and the NLO-accurate Drell-Yan ones scales as α^2 , resulting in a relative difference with respect to the target of the order of 0.1%, as shown in the last column of Table 3. Since the PDFs in this case were evolved using a consistently modified α , one cannot expect the scaling of the effects to be determined exactly by the ratio of the α values used. Nevertheless, it is possible to observe that the numbers in the last column of Table 3 scale approximately as the square of the ratio of the α values, when compared to those in the last column of

Table 2.

With a view to jointly addressing combined QCD and QED corrections, the QCD theory would constrain the choice of p_T^c to values no smaller than ~ 1 GeV. We can therefore take the results corresponding to $p_T^c \sim 1$ GeV (next-to-last row in Table 3) as a reasonable estimate of the accuracy of the MiNLO method variant. We can then conclude this section by saying that, by applying the MiNLO method as presented in this paper, we get an accuracy within the 0.01% between MiNLO and the NLO target, for a realistic choice of the value of the QED coupling α .

6 Conclusions

The electroweak physics program at the (HL-)LHC, particularly the precision measurements based on template fits to Drell-Yan processes, demands Monte Carlo tools that incorporate frontier calculations of both QCD and EW radiative corrections to minimize theoretical systematic uncertainties. Currently, state-of-the-art event generators for Drell-Yan production achieve NNLO + parton shower (PS) accuracy in QCD, while EW effects are available in generators featuring NLO QCD + NLO EW accuracy matched to QED and QCD parton showers for the inclusive process. On one hand, a framework capable of simultaneously treating NNLO QCD and NLO EW corrections matched to their respective parton showers is still missing. On the other hand, no tool currently provides NLO EW+PS accuracy for both the inclusive process and DY production in association with resolved radiation. This latter aspect is becoming increasingly important as the growing LHC statistics allow experimental collaborations to perform differential measurements over radiation-sensitive variables, such as the vector-boson transverse momentum.

The MiNNLO_{PS} method, designed to achieve NNLO QCD accuracy for an inclusive process, starting from the simulation of the corresponding radiative process at NLO, represents a natural starting point for developing a DY event generator with NNLO QCD + NLO EW + PS accuracy.

In this work, we take the first steps in this direction by presenting a possible formulation of the MiNLO method for QED corrections. We follow the original QCD formulation of MiNLO as closely as possible to highlight the specific features that arise in the QED case. To this end, we adopted $pp \rightarrow Z(\rightarrow \nu\bar{\nu})$ as the inclusive reference process, in order to have only initial-state radiation effects. We start from the QED corrections to $pp \rightarrow Z\mathcal{A}$ (with $\mathcal{A} = \gamma, q, \bar{q}$), including both quark and photon-initiated processes. We have presented the abelianization of the MiNLO formulae and we have shown that the modified couplings and coefficients in the Sudakov form factor have a deep impact on the position of its peak, locating it at such a small value of the transverse momentum of the vector boson, where any numerical evaluation of the corresponding amplitudes turns out to be totally unreliable. To address this issue, we proposed a strategy for the computation of the small

transverse-momentum differential cross section, exploiting the analytical properties of the MiNLO formula. This led to the introduction of a technical cutoff, p_T^c , that we have used to separate the differential cross section into two contributions, neglecting power-suppressed terms in the small transverse-momentum region.

In addition, we have discussed the treatment of the coupling associated with radiative emission and the repercussions of the running of electromagnetic coupling α on the calculation of the radiative corrections. We have addressed the role of the parton distribution functions and the interplay between the QED evolution of the PDFs and the MiNLO formulae. We have presented the validation of the method, along with several numerical results, in the setup featuring only the first-generation of quarks and an enhanced value of the electromagnetic coupling, in order to emphasize physical effects and potential discrepancies with respect to the expected behavior of the MiNLO formulae.

We have also quantified the uncertainties on the inclusive predictions arising from the proposed formalism and missing PDF evolution terms, when using a realistic value for α . We have studied the dependence of the differential cross section on the technical cut p_T^c , and we have found that, for values of p_T^c of the order of 1 GeV (typical cutoff value in the QCD MiNLO applications), the uncertainty is at the 0.01% level, for initial-state radiation effects.

The study presented here is a necessary first step towards incorporating full EW effects into the MiNNLO_{PS} framework. Future developments will involve extending this approach to final-state radiation, building upon the MiNLO formulation for $t\bar{t}$ production, achieving a combined treatment of QCD and QED corrections and, finally, exploring the strategies to incorporate full electroweak effects beyond the pure QED approximation.

Acknowledgments

We would like to thank L. Buonocore, A. Denner, G. Ferrera, J. Lindert, P.F. Monni, P. Nason, L. Rottoli, P. Torrielli and S. Uccirati for useful discussions, and C. Davies for providing us with a copy of her PhD thesis. We would also like to thank V. Bertone and S. Carrazza for exchanges about the APFEL code. F.B. and M.C. would like to thank the kind hospitality of the GGI Institute in Florence, Italy, during part of the work.

This work has been partially supported by the Italian Ministry of University and Research (MUR), with EU funds (NextGenerationEU), through the PRIN2022 grant agreement Nr. 20229KEFAM (CUP H53D23000980006, I53D23001000006).

This work is also partially supported by ICSC - Centro Nazionale di Ricerca in High Performance Computing, Big Data and Quantum Computing, funded by European Union - NextGenerationEU.

References

- [1] CMS collaboration, A. Hayrapetyan et al., *Measurement of the Drell–Yan forward-backward asymmetry and of the effective leptonic weak mixing angle in proton-proton collisions at $\sqrt{s} = 13$ TeV*, *Phys. Lett. B* **866** (2025) 139526 [[2408.07622](#)].
- [2] ATLAS collaboration, G. Aad et al., *Measurement of the forward-backward asymmetry of electron and muon pair-production in pp collisions at $\sqrt{s} = 7$ TeV with the ATLAS detector*, *JHEP* **09** (2015) 049 [[1503.03709](#)].
- [3] LHCb collaboration, R. Aaij et al., *Measurement of the forward-backward asymmetry in $Z/\gamma^* \rightarrow \mu^+ \mu^-$ decays and determination of the effective weak mixing angle*, *JHEP* **11** (2015) 190 [[1509.07645](#)].
- [4] ATLAS collaboration, G. Aad et al., *Measurement of the W-boson mass and width with the ATLAS detector using proton–proton collisions at $\sqrt{s} = 7$ TeV*, *Eur. Phys. J. C* **84** (2024) 1309 [[2403.15085](#)].
- [5] CMS collaboration, V. Chekhovsky et al., *High-precision measurement of the W boson mass with the CMS experiment at the LHC*, [2412.13872](#).
- [6] A. Denner and S. Dittmaier, *Electroweak Radiative Corrections for Collider Physics*, *Phys. Rept.* **864** (2020) 1 [[1912.06823](#)].
- [7] S. Dittmaier and M. Krämer, *Electroweak radiative corrections to W boson production at hadron colliders*, *Phys. Rev. D* **65** (2002) 073007 [[hep-ph/0109062](#)].
- [8] U. Baur and D. Wackerth, *Electroweak radiative corrections to $p\bar{p} \rightarrow W^\pm \rightarrow \ell^\pm \nu$ beyond the pole approximation*, *Phys. Rev. D* **70** (2004) 073015 [[hep-ph/0405191](#)].
- [9] V. A. Zykunov, *Radiative corrections to the Drell-Yan process at large dilepton invariant masses*, *Phys. Atom. Nucl.* **69** (2006) 1522.
- [10] A. Arbuzov, D. Bardin, S. Bondarenko, P. Christova, L. Kalinovskaya, G. Nanava et al., *One-loop corrections to the Drell-Yan process in SANC. I. The Charged current case*, *Eur. Phys. J. C* **46** (2006) 407 [[hep-ph/0506110](#)].
- [11] C. M. Carloni Calame, G. Montagna, O. Nicrosini and A. Vicini, *Precision electroweak calculation of the charged current Drell-Yan process*, *JHEP* **12** (2006) 016 [[hep-ph/0609170](#)].
- [12] U. Baur, O. Brein, W. Hollik, C. Schappacher and D. Wackerth, *Electroweak radiative corrections to neutral current Drell-Yan processes at hadron colliders*, *Phys. Rev. D* **65** (2002) 033007 [[hep-ph/0108274](#)].
- [13] V. A. Zykunov, *Weak radiative corrections to Drell-Yan process for large invariant mass of di-lepton pair*, *Phys. Rev. D* **75** (2007) 073019 [[hep-ph/0509315](#)].
- [14] C. M. Carloni Calame, G. Montagna, O. Nicrosini and A. Vicini, *Precision electroweak calculation of the production of a high transverse-momentum lepton pair at hadron colliders*, *JHEP* **10** (2007) 109 [[0710.1722](#)].

[15] A. Arbuzov, D. Bardin, S. Bondarenko, P. Christova, L. Kalinovskaya, G. Nanava et al., *One-loop corrections to the Drell–Yan process in SANC. (II). The Neutral current case*, *Eur. Phys. J. C* **54** (2008) 451 [[0711.0625](#)].

[16] S. Dittmaier and M. Huber, *Radiative corrections to the neutral-current Drell-Yan process in the Standard Model and its minimal supersymmetric extension*, *JHEP* **01** (2010) 060 [[0911.2329](#)].

[17] U. Baur, S. Keller and D. Wackerlo, *Electroweak radiative corrections to W boson production in hadronic collisions*, *Phys. Rev. D* **59** (1999) 013002 [[hep-ph/9807417](#)].

[18] W. Placzek and S. Jadach, *Multiphoton radiation in leptonic W boson decays*, *Eur. Phys. J. C* **29** (2003) 325 [[hep-ph/0302065](#)].

[19] C. M. Carloni Calame, G. Montagna, O. Nicrosini and M. Treccani, *Higher order QED corrections to W boson mass determination at hadron colliders*, *Phys. Rev. D* **69** (2004) 037301 [[hep-ph/0303102](#)].

[20] S. Bremsing, S. Dittmaier, M. Krämer and A. Mück, *Radiative corrections to W^- boson hadroproduction: Higher-order electroweak and supersymmetric effects*, *Phys. Rev. D* **77** (2008) 073006 [[0710.3309](#)].

[21] U. Baur, S. Keller and W. K. Sakumoto, *QED radiative corrections to Z boson production and the forward backward asymmetry at hadron colliders*, *Phys. Rev. D* **57** (1998) 199 [[hep-ph/9707301](#)].

[22] A. Andonov, A. Arbuzov, D. Bardin, S. Bondarenko, P. Christova, L. Kalinovskaya et al., *Standard SANC Modules*, *Comput. Phys. Commun.* **181** (2010) 305 [[0812.4207](#)].

[23] D. Bardin, S. Bondarenko, P. Christova, L. Kalinovskaya, L. Rumyantsev, A. Sapronov et al., *SANC integrator in the progress: QCD and EW contributions*, *JETP Lett.* **96** (2012) 285 [[1207.4400](#)].

[24] S. G. Bondarenko and A. A. Sapronov, *NLO EW and QCD proton-proton cross section calculations with mcsanc-v1.01*, *Comput. Phys. Commun.* **184** (2013) 2343 [[1301.3687](#)].

[25] A. Arbuzov, D. Bardin, S. Bondarenko, P. Christova, L. Kalinovskaya, U. Klein et al., *Update of the MCSANC Monte Carlo integrator, v. 1.20*, *JETP Lett.* **103** (2016) 131 [[1509.03052](#)].

[26] A. Arbuzov, D. Bardin, S. Bondarenko, P. Christova, L. Kalinovskaya, R. Sadykov et al., *Computer system SANC: its development and applications*, *J. Phys. Conf. Ser.* **762** (2016) 012062.

[27] A. Arbuzov, S. Bondarenko, Y. Dydyyshka, L. Kalinovskaya, R. Sadykov, V. Yermolchyk et al., *Electroweak Effects in Neutral Current Drell–Yan Processes within SANC System*, *Phys. Part. Nucl.* **54** (2023) 552 [[2212.05292](#)].

[28] J. M. Campbell, D. Wackeroth and J. Zhou, *Study of weak corrections to Drell-Yan, top-quark pair, and dijet production at high energies with MCFM*, *Phys. Rev. D* **94** (2016) 093009 [[1608.03356](#)].

[29] J. Alwall, R. Frederix, S. Frixione, V. Hirschi, F. Maltoni, O. Mattelaer et al., *The automated computation of tree-level and next-to-leading order differential cross sections, and their matching to parton shower simulations*, *JHEP* **07** (2014) 079 [[1405.0301](#)].

[30] R. Frederix, S. Frixione, V. Hirschi, D. Pagani, H. S. Shao and M. Zaro, *The automation of next-to-leading order electroweak calculations*, *JHEP* **07** (2018) 185 [[1804.10017](#)].

[31] B. Biedermann, S. Bräuer, A. Denner, M. Pellen, S. Schumann and J. M. Thompson, *Automation of NLO QCD and EW corrections with Sherpa and Recola*, *Eur. Phys. J. C* **77** (2017) 492 [[1704.05783](#)].

[32] SHERPA collaboration, E. Bothmann et al., *Event generation with Sherpa 3*, *JHEP* **12** (2024) 156 [[2410.22148](#)].

[33] S. Alioli et al., *Precision studies of observables in $pp \rightarrow W \rightarrow l\nu_l$ and $pp \rightarrow \gamma, Z \rightarrow l^+l^-$ processes at the LHC*, *Eur. Phys. J. C* **77** (2017) 280 [[1606.02330](#)].

[34] Y. Li and F. Petriello, *Combining QCD and electroweak corrections to dilepton production in FEWZ*, *Phys. Rev. D* **86** (2012) 094034 [[1208.5967](#)].

[35] M. Grazzini, S. Kallweit and M. Wiesemann, *Fully differential NNLO computations with MATRIX*, *Eur. Phys. J. C* **78** (2018) 537 [[1711.06631](#)].

[36] L. Buonocore, M. Grazzini and F. Tramontano, *The q_T subtraction method: electroweak corrections and power suppressed contributions*, *Eur. Phys. J. C* **80** (2020) 254 [[1911.10166](#)].

[37] M. Grazzini, S. Kallweit, J. M. Lindert, S. Pozzorini and M. Wiesemann, *NNLO QCD + NLO EW with Matrix+OpenLoops: precise predictions for vector-boson pair production*, *JHEP* **02** (2020) 087 [[1912.00068](#)].

[38] L. Chen and A. Freitas, *GRiffin: A C++ library for electroweak radiative corrections in fermion scattering and decay processes*, *SciPost Phys. Codeb.* **2023** (2023) 18 [[2211.16272](#)].

[39] S. Jadach, B. F. L. Ward, Z. A. Was and S. A. Yost, *KK MC-hh: Resummed exact $\mathcal{O}(\alpha^2 L)$ EW corrections in a hadronic MC event generator*, *Phys. Rev. D* **94** (2016) 074006 [[1608.01260](#)].

[40] S. Jadach, B. F. L. Ward, Z. A. Was and S. A. Yost, *Systematic Studies of Exact $\mathcal{O}(\alpha^2 L)$ CEEX EW Corrections in a Hadronic MC for Precision Z/γ^* Physics at LHC Energies*, *Phys. Rev. D* **99** (2019) 076016 [[1707.06502](#)].

[41] S. A. Yost, J. Stanislaw, B. F. L. Ward and W. Zbigniew, *ISR and IFI in Precision AFB Studies with KKMC-hh*, *PoS RADCOR2019* (2019) 085 [[2002.12477](#)].

[42] S. A. Yost, M. Dittrich, S. Jadach, B. F. L. Ward and Z. Was, *KKMC-hh for Precision Electroweak Phenomenology at the LHC*, *PoS ICHEP2020* (2021) 349 [[2012.09298](#)].

[43] S. A. Yost, S. Jadach, B. F. L. Ward and Z. Was, *KKMChh: Matching CEE_X Photonic ISR to a QED-Corrected Parton Shower*, *PoS ICHEP2022* (2022) 887 [[2211.17177](#)].

[44] M. Delto, M. Jaquier, K. Melnikov and R. Röntsch, *Mixed QCD \otimes QED corrections to on-shell Z boson production at the LHC*, *JHEP* **01** (2020) 043 [[1909.08428](#)].

[45] L. Cieri, D. de Florian, M. Der and J. Mazzitelli, *Mixed QCD \otimes QED corrections to exclusive Drell Yan production using the q_T -subtraction method*, *JHEP* **09** (2020) 155 [[2005.01315](#)].

[46] R. Bonciani, F. Buccioni, R. Mondini and A. Vicini, *Double-real corrections at $\mathcal{O}(\alpha\alpha_s)$ to single gauge boson production*, *Eur. Phys. J. C* **77** (2017) 187 [[1611.00645](#)].

[47] R. Bonciani, F. Buccioni, N. Rana, I. Triscari and A. Vicini, *NNLO QCD \times EW corrections to Z production in the $q\bar{q}$ channel*, *Phys. Rev. D* **101** (2020) 031301 [[1911.06200](#)].

[48] R. Bonciani, F. Buccioni, N. Rana and A. Vicini, *Next-to-Next-to-Leading Order Mixed QCD-Electroweak Corrections to on-Shell Z Production*, *Phys. Rev. Lett.* **125** (2020) 232004 [[2007.06518](#)].

[49] R. Bonciani, F. Buccioni, N. Rana and A. Vicini, *On-shell Z boson production at hadron colliders through $\mathcal{O}(\alpha\alpha_s)$* , *JHEP* **02** (2022) 095 [[2111.12694](#)].

[50] F. Buccioni, F. Caola, M. Delto, M. Jaquier, K. Melnikov and R. Röntsch, *Mixed QCD-electroweak corrections to on-shell Z production at the LHC*, *Phys. Lett. B* **811** (2020) 135969 [[2005.10221](#)].

[51] A. Behring, F. Buccioni, F. Caola, M. Delto, M. Jaquier, K. Melnikov et al., *Mixed QCD-electroweak corrections to W-boson production in hadron collisions*, *Phys. Rev. D* **103** (2021) 013008 [[2009.10386](#)].

[52] S. Dittmaier, A. Huss and C. Schwinn, *Mixed QCD-electroweak $\mathcal{O}(\alpha_s\alpha)$ corrections to Drell-Yan processes in the resonance region: pole approximation and non-factorizable corrections*, *Nucl. Phys. B* **885** (2014) 318 [[1403.3216](#)].

[53] S. Dittmaier, A. Huss and C. Schwinn, *Dominant mixed QCD-electroweak $\mathcal{O}(\alpha_s\alpha)$ corrections to Drell-Yan processes in the resonance region*, *Nucl. Phys. B* **904** (2016) 216 [[1511.08016](#)].

[54] S. Dittmaier, T. Schmidt and J. Schwarz, *Mixed NNLO QCD \times electroweak corrections of $\mathcal{O}(N_f\alpha_s\alpha)$ to single-W/Z production at the LHC*, *JHEP* **12** (2020) 201 [[2009.02229](#)].

[55] S. Dittmaier, A. Huss and J. Schwarz, *Mixed NNLO QCD \times electroweak*

corrections to single- Z production in pole approximation: differential distributions and forward-backward asymmetry, [JHEP 05 \(2024\) 170 \[2401.15682\]](#).

[56] D. de Florian, M. Der and I. Fabre, *$QCD \oplus QED$ NNLO corrections to Drell Yan production*, [Phys. Rev. D 98 \(2018\) 094008 \[1805.12214\]](#).

[57] R. Bonciani, L. Buonocore, M. Grazzini, S. Kallweit, N. Rana, F. Tramontano et al., *Mixed Strong-Electroweak Corrections to the Drell-Yan Process*, [Phys. Rev. Lett. 128 \(2022\) 012002 \[2106.11953\]](#).

[58] F. Buccioni, F. Caola, H. A. Chawdhry, F. Devoto, M. Heller, A. von Manteuffel et al., *Mixed QCD-electroweak corrections to dilepton production at the LHC in the high invariant mass region*, [JHEP 06 \(2022\) 022 \[2203.11237\]](#).

[59] T. Armadillo, R. Bonciani, S. Devoto, N. Rana and A. Vicini, *Two-loop mixed QCD-EW corrections to neutral current Drell-Yan*, [JHEP 05 \(2022\) 072 \[2201.01754\]](#).

[60] L. Buonocore, M. Grazzini, S. Kallweit, C. Savoini and F. Tramontano, *Mixed QCD-EW corrections to $pp \rightarrow \ell\nu_\ell + X$ at the LHC*, [Phys. Rev. D 103 \(2021\) 114012 \[2102.12539\]](#).

[61] T. Armadillo, R. Bonciani, S. Devoto, N. Rana and A. Vicini, *Two-loop mixed QCD-EW corrections to charged current Drell-Yan*, [JHEP 07 \(2024\) 265 \[2405.00612\]](#).

[62] A. Behring, F. Buccioni, F. Caola, M. Delto, M. Jaquier, K. Melnikov et al., *Estimating the impact of mixed QCD-electroweak corrections on the W -mass determination at the LHC*, [Phys. Rev. D 103 \(2021\) 113002 \[2103.02671\]](#).

[63] T. Armadillo, S. Devoto, M. Dradi and A. Vicini, *Towards the two-loop electroweak corrections to the Drell-Yan process: the infrared structure*, [2511.20365](#).

[64] L. Cieri, G. Ferrera and G. F. R. Sborlini, *Combining QED and QCD transverse-momentum resummation for Z boson production at hadron colliders*, [JHEP 08 \(2018\) 165 \[1805.11948\]](#).

[65] A. Autieri, L. Cieri, G. Ferrera and G. F. R. Sborlini, *Combining QED and QCD transverse-momentum resummation for W and Z boson production at hadron colliders*, [JHEP 07 \(2023\) 104 \[2302.05403\]](#).

[66] L. Buonocore, L. Rottoli and P. Torrielli, *Resummation of combined QCD-electroweak effects in Drell Yan lepton-pair production*, [JHEP 07 \(2024\) 193 \[2404.15112\]](#).

[67] A. Autieri, S. Camarda, L. Cieri, G. Ferrera and G. Sborlini, *Transverse-momentum resummation at mixed $QCD \otimes QED$ NNLL accuracy for Z boson production at hadron colliders*, [2511.07324](#).

[68] G. Billis, F. J. Tackmann and J. Talbert, *Higher-Order Sudakov Resummation in Coupled Gauge Theories*, [JHEP 03 \(2020\) 182 \[1907.02971\]](#).

[69] P. Nason, *A New method for combining NLO QCD with shower Monte Carlo algorithms*, *JHEP* **11** (2004) 040 [[hep-ph/0409146](#)].

[70] S. Frixione, P. Nason and C. Oleari, *Matching NLO QCD computations with Parton Shower simulations: the POWHEG method*, *JHEP* **11** (2007) 070 [[0709.2092](#)].

[71] S. Alioli, P. Nason, C. Oleari and E. Re, *A general framework for implementing NLO calculations in shower Monte Carlo programs: the POWHEG BOX*, *JHEP* **06** (2010) 043 [[1002.2581](#)].

[72] T. Ježo and P. Nason, *On the Treatment of Resonances in Next-to-Leading Order Calculations Matched to a Parton Shower*, *JHEP* **12** (2015) 065 [[1509.09071](#)].

[73] S. Frixione and B. R. Webber, *Matching NLO QCD computations and parton shower simulations*, *JHEP* **06** (2002) 029 [[hep-ph/0204244](#)].

[74] J. Bellm et al., *Herwig 7.0/Herwig++ 3.0 release note*, *Eur. Phys. J. C* **76** (2016) 196 [[1512.01178](#)].

[75] S. Platzer and S. Gieseke, *Dipole Showers and Automated NLO Matching in Herwig++*, *Eur. Phys. J. C* **72** (2012) 2187 [[1109.6256](#)].

[76] S. Hoeche, F. Krauss, M. Schonherr and F. Siegert, *A critical appraisal of NLO+PS matching methods*, *JHEP* **09** (2012) 049 [[1111.1220](#)].

[77] SHERPA collaboration, E. Bothmann et al., *Event Generation with Sherpa 2.2*, *SciPost Phys.* **7** (2019) 034 [[1905.09127](#)].

[78] C. W. Bauer, F. J. Tackmann and J. Thaler, *GenEvA. I. A New framework for event generation*, *JHEP* **12** (2008) 010 [[0801.4026](#)].

[79] S. Alioli, C. W. Bauer, C. Berggren, F. J. Tackmann, J. R. Walsh and S. Zuberi, *Matching Fully Differential NNLO Calculations and Parton Showers*, *JHEP* **06** (2014) 089 [[1311.0286](#)].

[80] S. Kallweit, J. M. Lindert, P. Maierhofer, S. Pozzorini and M. Schönherr, *NLO QCD+EW predictions for $V + \text{jets}$ including off-shell vector-boson decays and multijet merging*, *JHEP* **04** (2016) 021 [[1511.08692](#)].

[81] C. Gütschow, J. M. Lindert and M. Schönherr, *Multi-jet merged top-pair production including electroweak corrections*, *Eur. Phys. J. C* **78** (2018) 317 [[1803.00950](#)].

[82] S. Bräuer, A. Denner, M. Pellen, M. Schönherr and S. Schumann, *Fixed-order and merged parton-shower predictions for WW and WWj production at the LHC including NLO QCD and EW corrections*, *JHEP* **10** (2020) 159 [[2005.12128](#)].

[83] J. M. Lindert, D. Lombardi, M. Wiesemann, G. Zanderighi and S. Zanoli, *$W^\pm Z$ production at NNLO QCD and NLO EW matched to parton showers with MiNNLO_{PS}*, *JHEP* **11** (2022) 036 [[2208.12660](#)].

[84] L. Barzè, G. Montagna, P. Nason, O. Nicrosini and F. Piccinini, *Implementation of electroweak corrections in the POWHEG BOX: single W production*, *JHEP* **04** (2012) 037 [[1202.0465](#)].

[85] C. Bernaciak and D. Wackerlo, *Combining NLO QCD and Electroweak Radiative Corrections to W boson Production at Hadron Colliders in the POWHEG Framework*, *Phys. Rev. D* **85** (2012) 093003 [[1201.4804](#)].

[86] L. Barzè, G. Montagna, P. Nason, O. Nicrosini, F. Piccinini and A. Vicini, *Neutral current Drell-Yan with combined QCD and electroweak corrections in the POWHEG BOX*, *Eur. Phys. J. C* **73** (2013) 2474 [[1302.4606](#)].

[87] A. Mück and L. Oymanns, *Resonance-improved parton-shower matching for the Drell-Yan process including electroweak corrections*, *JHEP* **05** (2017) 090 [[1612.04292](#)].

[88] M. Chiesa, F. Piccinini and A. Vicini, *Direct determination of $\sin^2 \theta_{eff}^\ell$ at hadron colliders*, *Phys. Rev. D* **100** (2019) 071302 [[1906.11569](#)].

[89] F. Granata, J. M. Lindert, C. Oleari and S. Pozzorini, *NLO QCD+EW predictions for HV and HV + jet production including parton-shower effects*, *JHEP* **09** (2017) 012 [[1706.03522](#)].

[90] M. Chiesa, C. Oleari and E. Re, *NLO QCD+NLO EW corrections to diboson production matched to parton shower*, *Eur. Phys. J. C* **80** (2020) 849 [[2005.12146](#)].

[91] B. Jäger and J. Scheller, *Electroweak corrections and shower effects to Higgs production in association with two jets at the LHC*, *JHEP* **09** (2022) 191 [[2208.00013](#)].

[92] M. Chiesa, A. Denner, J.-N. Lang and M. Pellen, *An event generator for same-sign W-boson scattering at the LHC including electroweak corrections*, *Eur. Phys. J. C* **79** (2019) 788 [[1906.01863](#)].

[93] C. M. Carloni Calame, M. Chiesa, H. Martinez, G. Montagna, O. Nicrosini, F. Piccinini et al., *Precision Measurement of the W-Boson Mass: Theoretical Contributions and Uncertainties*, *Phys. Rev. D* **96** (2017) 093005 [[1612.02841](#)].

[94] L. Barzè, M. Chiesa, G. Montagna, P. Nason, O. Nicrosini, F. Piccinini et al., *$W\gamma$ production in hadronic collisions using the POWHEG+MiNLO method*, *JHEP* **12** (2014) 039 [[1408.5766](#)].

[95] T. Jezo, M. Klasen and F. König, *Prompt photon production and photon-hadron jet correlations with POWHEG*, *JHEP* **11** (2016) 033 [[1610.02275](#)].

[96] D. Lombardi, M. Wiesemann and G. Zanderighi, *Advancing MiNNLO_{PS} to diboson processes: $Z\gamma$ production at NNLO+PS*, *JHEP* **06** (2021) 095 [[2010.10478](#)].

[97] T. Cridge, M. A. Lim and R. Nagar, *$W\gamma$ production at NNLO+PS accuracy in Geneva*, *Phys. Lett. B* **826** (2022) 136918 [[2105.13214](#)].

[98] A. Gavardi, C. Oleari and E. Re, *NNLO+PS Monte Carlo simulation of photon pair production with MiNNLO_{PS}*, *JHEP* **09** (2022) 061 [[2204.12602](#)].

[99] A. Denner, S. Dittmaier, M. Hecht and C. Pasold, *NLO QCD and electroweak corrections to $W + \gamma$ production with leptonic W-boson decays*, *JHEP* **04** (2015) 018 [[1412.7421](#)].

[100] A. Denner, S. Dittmaier, M. Hecht and C. Pasold, *NLO QCD and electroweak corrections to $Z + \gamma$ production with leptonic Z -boson decays*, *JHEP* **02** (2016) 057 [[1510.08742](#)].

[101] K. Hamilton, P. Nason, C. Oleari and G. Zanderighi, *Merging $H/W/Z + 0$ and 1 jet at NLO with no merging scale: a path to parton shower + NNLO matching*, *JHEP* **05** (2013) 082 [[1212.4504](#)].

[102] K. Hamilton, P. Nason and G. Zanderighi, *MINLO: Multi-Scale Improved NLO*, *JHEP* **10** (2012) 155 [[1206.3572](#)].

[103] P. F. Monni, P. Nason, E. Re, M. Wiesemann and G. Zanderighi, *MiNNLO_{PS}: a new method to match NNLO QCD to parton showers*, *JHEP* **05** (2020) 143 [[1908.06987](#)].

[104] P. F. Monni, E. Re and M. Wiesemann, *MiNNLO_{PS}: optimizing $2 \rightarrow 1$ hadronic processes*, *Eur. Phys. J. C* **80** (2020) 1075 [[2006.04133](#)].

[105] J. Mazzitelli, P. F. Monni, P. Nason, E. Re, M. Wiesemann and G. Zanderighi, *Next-to-Next-to-Leading Order Event Generation for Top-Quark Pair Production*, *Phys. Rev. Lett.* **127** (2021) 062001 [[2012.14267](#)].

[106] J. Mazzitelli, A. Ratti, M. Wiesemann and G. Zanderighi, *B-hadron production at the LHC from bottom-quark pair production at NNLO+PS*, *Phys. Lett. B* **843** (2023) 137991 [[2302.01645](#)].

[107] J. Mazzitelli, V. Sotnikov and M. Wiesemann, *Next-to-next-to-leading order event generation for Z -boson production in association with a bottom-quark pair*, *Phys. Rev. D* **112** (2025) 056031 [[2404.08598](#)].

[108] C. Biello, J. Mazzitelli, A. Sankar, M. Wiesemann and G. Zanderighi, *Higgs boson production in association with massive bottom quarks at NNLO+PS*, *JHEP* **04** (2025) 088 [[2412.09510](#)].

[109] K. Hamilton, P. Nason, E. Re and G. Zanderighi, *NNLO_{PS} simulation of Higgs boson production*, *JHEP* **10** (2013) 222 [[1309.0017](#)].

[110] S. Höche, Y. Li and S. Prestel, *Drell-Yan lepton pair production at NNLO QCD with parton showers*, *Phys. Rev. D* **91** (2015) 074015 [[1405.3607](#)].

[111] S. Höche, Y. Li and S. Prestel, *Higgs-boson production through gluon fusion at NNLO QCD with parton showers*, *Phys. Rev. D* **90** (2014) 054011 [[1407.3773](#)].

[112] J. Mazzitelli, P. F. Monni, P. Nason, E. Re, M. Wiesemann and G. Zanderighi, *Top-pair production at the LHC with MINNLO_{PS}*, *JHEP* **04** (2022) 079 [[2112.12135](#)].

[113] S. Kallweit, J. M. Lindert, S. Pozzorini and M. Schönherr, *NLO QCD+EW predictions for $2\ell 2\nu$ diboson signatures at the LHC*, *JHEP* **11** (2017) 120 [[1705.00598](#)].

[114] S. Frixione, Z. Kunszt and A. Signer, *Three jet cross-sections to next-to-leading order*, *Nucl. Phys. B* **467** (1996) 399 [[hep-ph/9512328](#)].

[115] S. Frixione, *A General approach to jet cross-sections in QCD*, *Nucl. Phys. B* **507** (1997) 295 [[hep-ph/9706545](#)].

[116] J. Erler, *Calculation of the QED coupling $\hat{\alpha}(M_Z)$ in the modified minimal subtraction scheme*, *Phys. Rev. D* **59** (1999) 054008 [[hep-ph/9803453](#)].

[117] S. Amoroso, M. Chiesa, C. L. Del Pio, K. Lipka, F. Piccinini, F. Vazzoler et al., *Probing the weak mixing angle at high energies at the LHC and HL-LHC*, *Phys. Lett. B* **844** (2023) 138103 [[2302.10782](#)].

[118] M. Chiesa, C. L. Del Pio and F. Piccinini, *On electroweak corrections to neutral current Drell-Yan with the POWHEG BOX*, *Eur. Phys. J. C* **84** (2024) 539 [[2402.14659](#)].

[119] G. P. Salam and J. Rojo, *A Higher Order Perturbative Parton Evolution Toolkit (HOPPET)*, *Comput. Phys. Commun.* **180** (2009) 120 [[0804.3755](#)].

[120] A. Karlberg, P. Nason, G. Salam, G. Zanderighi and F. Dreyer, *HOPPET v2 release note*, [2510.09310](#).

[121] A. Manohar, P. Nason, G. P. Salam and G. Zanderighi, *How bright is the proton? A precise determination of the photon parton distribution function*, *Phys. Rev. Lett.* **117** (2016) 242002 [[1607.04266](#)].

[122] A. V. Manohar, P. Nason, G. P. Salam and G. Zanderighi, *The Photon Content of the Proton*, *JHEP* **12** (2017) 046 [[1708.01256](#)].

[123] NNPDF collaboration, V. Bertone, S. Carrazza, N. P. Hartland and J. Rojo, *Illuminating the photon content of the proton within a global PDF analysis*, *SciPost Phys.* **5** (2018) 008 [[1712.07053](#)].

[124] A. Buckley, J. Ferrando, S. Lloyd, K. Nordström, B. Page, M. Rüfenacht et al., *LHAPDF6: parton density access in the LHC precision era*, *Eur. Phys. J. C* **75** (2015) 132 [[1412.7420](#)].

[125] S. Actis, A. Denner, L. Hofer, A. Scharf and S. Uccirati, *Recursive generation of one-loop amplitudes in the Standard Model*, *JHEP* **04** (2013) 037 [[1211.6316](#)].

[126] S. Actis, A. Denner, L. Hofer, J.-N. Lang, A. Scharf and S. Uccirati, *RECOLA: REcursive Computation of One-Loop Amplitudes*, *Comput. Phys. Commun.* **214** (2017) 140 [[1605.01090](#)].

[127] A. Denner, J.-N. Lang and S. Uccirati, *NLO electroweak corrections in extended Higgs Sectors with RECOLA2*, *JHEP* **07** (2017) 087 [[1705.06053](#)].

[128] A. Denner, J.-N. Lang and S. Uccirati, *Recola2: REcursive Computation of One-Loop Amplitudes 2*, *Comput. Phys. Commun.* **224** (2018) 346 [[1711.07388](#)].

[129] A. Denner, S. Dittmaier and L. Hofer, *Collier: a fortran-based Complex One-Loop Library in Extended Regularizations*, *Comput. Phys. Commun.* **212** (2017) 220 [[1604.06792](#)].

[130] A. Denner, *Techniques for calculation of electroweak radiative corrections at the*

one loop level and results for W physics at LEP-200, [Fortsch. Phys. 41 \(1993\) 307](#) [[0709.1075](#)].

[131] P. B. Arnold and R. P. Kauffman, *W and Z production at next-to-leading order: From large q_T to small*, [Nucl. Phys. B 349 \(1991\) 381](#).